A Luminescent NOTA-Based Terbium(III) "Turn-Off" Sensor for Copper

Clerc, Michèle ; Heinemann, Franz ; Spingler, Bernhard ; Gasser, Gilles

DOI: https://doi.org/10.1021/acs.inorgchem.9b02934

A Luminescent NOTA-based Terbium(III) 'Turn-Off' Sensor for Copper

Michèle Clerc,[a] Franz Heinemann,[a,b] Bernhard Spingler,[a]* and Gilles Gasser[b]*

[a] M. Clerc, F. Heinemann, Prof. Dr. B. Spingler
Department of Chemistry, University of Zurich
Winterthurerstrasse 190, CH-8057, Zurich, Switzerland
E-mail: spingler@chem.uzh.ch

[b] F. Heinemann, Dr. G. Gasser
Chimie ParisTech, PSL University, Laboratory for Inorganic Chemical Biology
F-75005 Paris, France
E-mail: gilles.gasser@chimieparistech.psl.eu
WWW: www.gassergroup.com

Abstract

A bimacrocyclic luminescent terbium(III) sensor is reported for the selective 'turn-off' detection of Cu^{2+} ions in aqueous solutions. The current sensor differentiates from previous sensors in that it offers the use of 1) time-gated luminescence detection to remove background signal, 2) a longer excitation wavelength of up to 350 nm for increased biocompatibility, and 3) a practically irreversible detection as a form of probing Cu^{2+} ions with an extremely low limit of detection of about 1.7 nM.

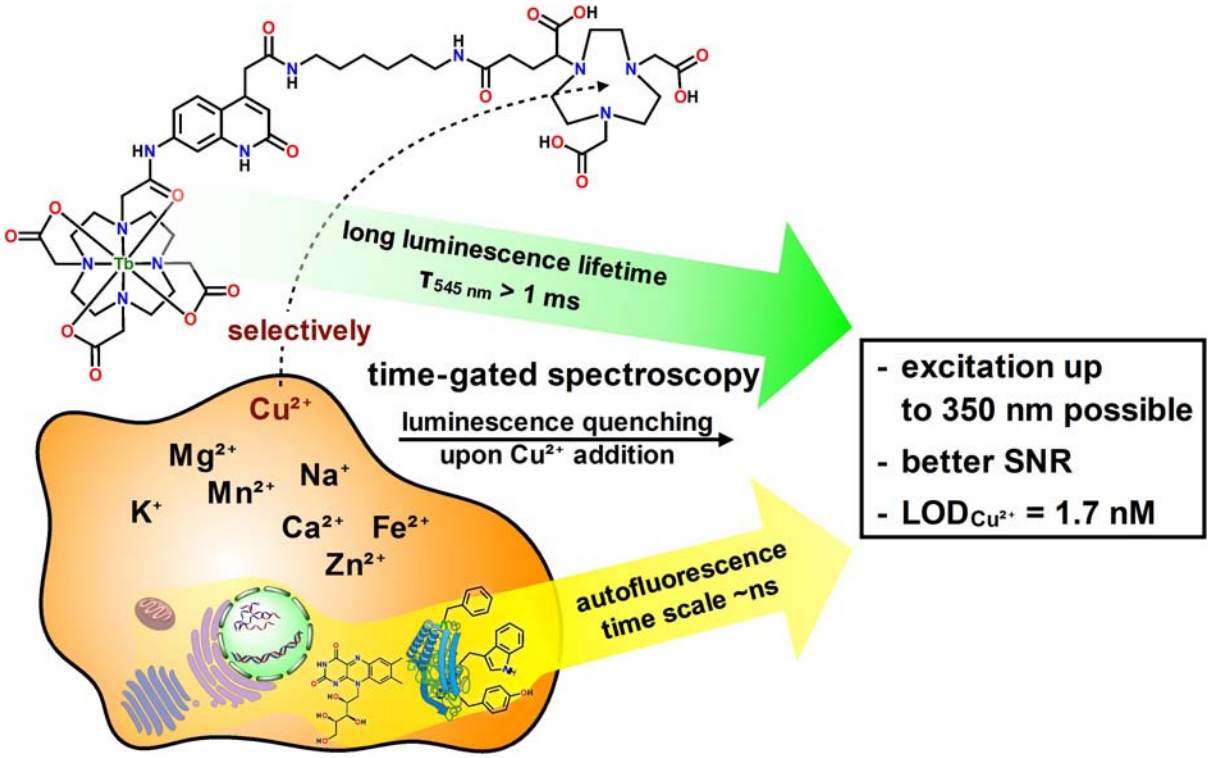

Synopsis: The detection of copper ions in aqueous solutions is an active and growing research field relevant to bioanalyses and environmental sampling. There is a high demand for sensitive and selective probes for copper in biological environment including intracellular monitoring. This would allow for a better understanding of the bivalent role of copper in the human body. Herein, we report a bimacrocyclic luminescent terbium(III) sensor for the selective 'turn-off' detection of Cu^{2+} ions in aqueous solutions.

Introduction

Copper being the third most abundant transition metal in the human body after iron and zinc is involved in various physiological and pathological processes.[1] As an important catalytic cofactor for many enzymatic reactions, copper plays a crucial role in cellular metabolism of all organisms.[2,3] A perturbed copper homeostasis was associated with numerous diseases, especially those related to brain function activity, including Menke's, Wilson's, Alzheimer's and Parkinson's disease, prion disorders and also cancer progression.[2–6]

As such, copper is both an essential micronutrient, but also toxic at low concentrations. Its rapid and precise detection in biological samples (e.g., blood, urine, brain microdialysates)[7,8] or environmental samples (e.g., fresh and waste water)[9–11] is therefore of paramount importance. Similarly, there is a demand for suitable probes in view of monitoring intracellular copper, including ion flux concentrations and transport, for a better understanding of the bivalent role of copper in the human body.[12–17] Current technologies for copper detection include atomic absorption spectrometry (AAS)[11], inductively coupled plasma-mass spectroscopy (ICP-MS)[7,18], surface plasmon resonance (SPR)[9,19], inductively coupled plasma-atomic emission spectrometry (ICP-AES)[20], electrochemical sensors[10,21] and light absorbance/emission-based techniques.[12,13,27–29,14–16,22–26] Luminescence-based chemosensors have the advantage of high sensitivity, rapid real-time response and accessibility from an economical perspective.

Copper shows high redox activity and can exist in three different oxidation states (Cu^0, Cu^+ and Cu^{2+}). Cu^{2+}ions are capable of luminescence quenching through an electron or energy transfer mechanism taking place from the luminescent molecule to the metal ion (or vice versa) and through paramagnetic effects.[30,31] This quenching ability is due to the Cu(II)'s unfilled $3d^9$ shell and has been exploited in the design of many fluorescence-based copper sensors.[26,30] An area of growing interest is the design of copper sensing probes that employ lanthanides, namely Tb(III) and Eu(III), due to their highly attractive photophysical properties (e.g., millisecond luminescence lifetimes, large Stokes shift, emission in the visible and sharp distinct emission bands, high photostability and low phototoxicity).[32,33] Designs of lanthanide probes for copper sensing include small molecule probes,[17–27] peptide mimics of metallo-protein binding sites,[45] nanoparticles,[8] and polymer-based materials.[46–50]

The most typical design for small molecule copper sensors based on lanthanides are compounds that contain sensitizer-receptor units, as for example seen in the sensor **S1**

reported by Gunnlaugsson *et al.* (Figure 1).[37] Here, the binding event causes changes to the photophysical properties of the sensitizer resulting in a modulation of the lanthanide luminescence signal. This can manifest itself, e.g., in quenched lifetimes of the energy states involved in the sensitization process or in diminished energy transfer rates from the sensitizer to the lanthanide as a result of alterations in the energy levels of the respective states.[51] Other sensors rely on more complex mechanisms. For example, the probes **S2** and **S3** were primarily reported for the reaction-based detection of H_2S/HS^-, but they also act as copper sensors exhibiting significant luminescence quenching upon binding of Cu^{2+} ions (Figure 1).[40,44] In the switch-like structure of **S2**, Cu^{2+} ion binding of the receptor moiety results in conformational change and coordination of the pyridine unit to Cu^{2+}, which then inhibits the energy transfer of the sensitizer to the lanthanide. The luminescence can be restored when Cu^{2+} is precipitated as CuS in the presence of the analyte H_2S to give a turn-on signal.[40] Other sensors make use of the disturbance of inbuilt photo-induced electron transfer (PeT) processes. For instance, Eliseeva *et al.* recently reported the turn-on Cu^{2+} ion sensor **S4** (Figure 1), for which the binding of Cu^{2+} ions suppresses a photon-induced electron transfer (PeT) quenching process taking place from the electron donating hydrazine moieties to the aromatic sensitizer.[41] In the process, Cu^{2+} is suggested to be partially reduced to Cu^+.[41] An irreversible reaction-based sensor includes the reaction pair **S5-1** and **S5-2** (Figure 1) reported by Hulme *et al.*, which detects Cu^+ ions through the copper-catalyzed alkyne-azide cycloaddition reaction (CuAAC) to produce **S5-3** (Figure 1) with a 'turn-on' luminescence signal.[35] This system is interesting as it is capable of reacting also with ligand-bound copper in native biological settings, as opposed to many reversible sensors for copper that cannot compete with copper-binding proteins.

Herein, we report a novel luminescent lanthanide-based sensor for the detection of nanomolar copper levels in aqueous solution. Our sensor comprises of a bimacrocylic structure including a luminescent Tb(III) moiety (**1**, Scheme 1) and a NOTA (1,4,7-triazacyclononane-1,4,7-triacetic acid) moiety for binding Cu^{2+} ions. For thermodynamic and kinetic reasons, H_3NOTA and other NOTA derivatives are widely used carriers of copper radionuclides as they predominantly form the Cu^{2+} complex over complexes with common impurities in radiochemical formulations, such as Zn^{2+} and Ni^{2+}.[52–54] As such, NOTA is an ideal receptor to trap Cu^{2+} ions in a fast and practically irreversible way at low concentrations and potentially even in the presence of biologically more abundant Zn^{2+}. Luminescent lanthanide complexes with carbostyril sensitizers are well known to possess high luminescence quantum

yields, millisecond lifetimes and excellent stability in aqueous solutions.[55,56] Further, the Tb(III) complex **1** is well water-soluble, relatively easy to synthesize and derivatize making it a suitable candidate for implementation into a sensor for aqueous conditions. Our planned design involves conformational flexibility to allow for the NOTA-bound Cu^{2+} moiety to interact with the carbostyril sensitizer to quench the Tb(III) luminescence and afford a 'turn-off' signal.

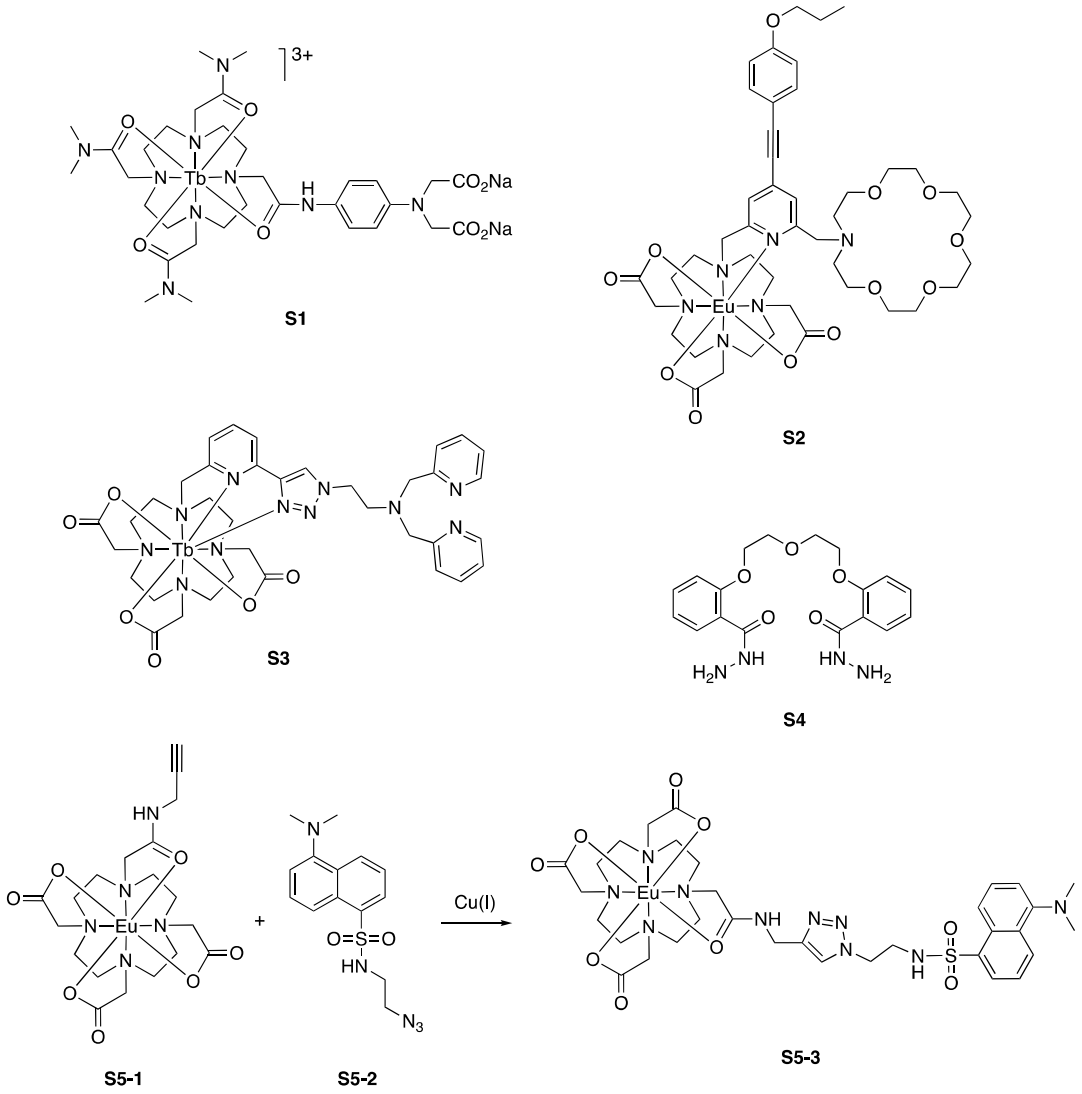

Figure 1. Lanthanide complexes for luminescence-based sensing of copper.

Results and Discussion

Syntheses

Compound **1** was prepared by following a reported procedure for the preparation of its Eu(III) analogue with the exception of the complexation step, which was performed with $Tb(OTf)_3$ instead of $Eu(OTf)_3$ to afford the respective Tb(III) complex (Scheme 1).[57,58] The next step involved the introduction of a 1,6-diaminohexane linker through a HATU-mediated amide condensation reaction to afford **2**. Compound **2** was then reacted with the *N*-hydroxysuccinimidyl activated ester (NHS ester), NODA-GA-NHS, in the presence of triethylamine in DMF to afford the final sensor compound **TCS1**. These compounds were characterized by mass spectrometry (LC-MS, HR-MS), IR and UV-Vis spectroscopy (Figures S5–S11). Elemental analysis was conducted for **1** and **TCS1** and ^{1}H-NMR and ^{13}C-NMR spectroscopy was performed for all intermediates in the synthesis of **1** (Figures S1–S4). For photophysical studies, the copper complex of **TCS1** (**TCS2**) was prepared *in situ* by addition of 1 equivalent of $CuCl_2$ to **TCS1** in unbuffered H_2O at room temperature.

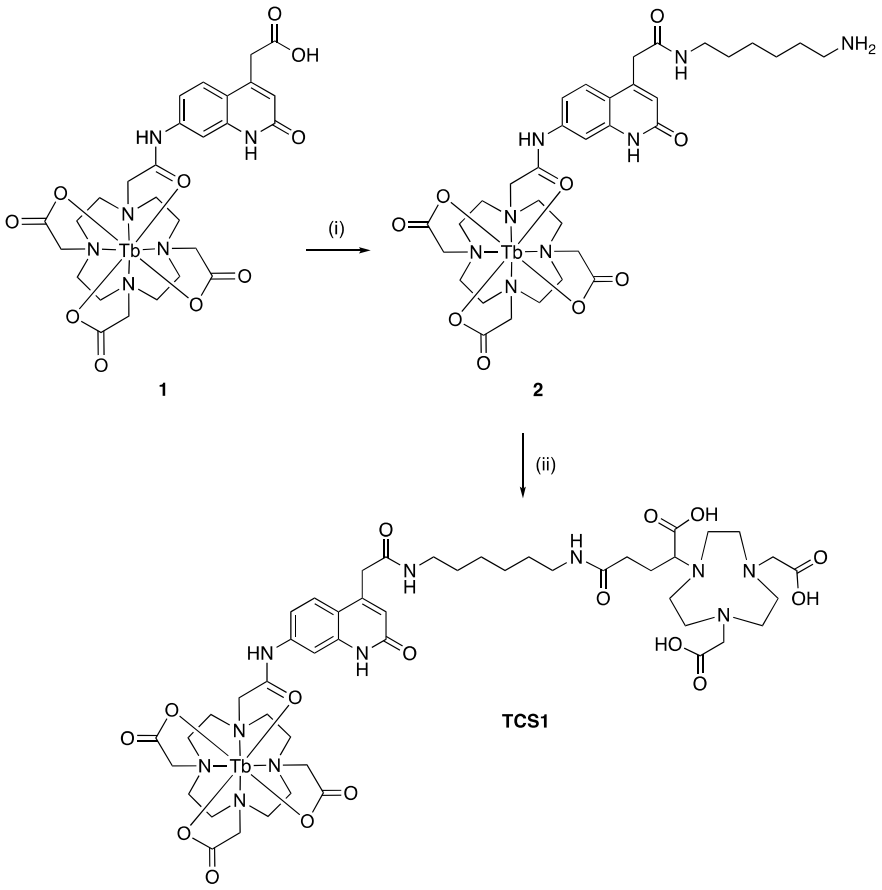

Scheme 1. Synthesis of Tb(III)-based copper sensor **TCS1**. Reaction conditions: (i) 1,6-Hexanediamine, HATU, Et_3N, DMSO, r.t., 17 h, 93%; (ii) NODA-GA-NHS ester, Et_3N, DMF, r.t., 20 h, 43%.

Photophysical investigation

First, we investigated the photophysical properties of **1**, **TCS1** and the copper complex **TCS2** to evaluate the viability of **TCS1** as a sensor for copper. As can be seen in Table 1, the absorption of **TCS1** extends into the longer UV region with excitation possible up to 350 nm (ε = 10 000 $M^{-1}cm^{-1}$ at λ = 347 nm, Figure S9). This offers an improvement over previous Tb(III)-based sensors for Cu^{2+} ions, which require excitation at ≤ 280 nm.[41,44] Excitation of **TCS1** results in long-lived metal-centered emission (four distinctive bands with maxima at 488, 545, 587 and 621 nm corresponding to transitions from the $^5D_4$ excited state to the ^7F_J (J = 6, 5, 4, 3) ground states) alongside residual sensitizer fluorescence that can be removed upon time resolution (Figure S10). The excitation spectrum resembles the absorbance spectrum of the carbostyril dye demonstrating that the Tb-centred emission is excited through the carbostyril sensitizer. **1** and **TCS1** are highly luminescent in aqueous solutions with lanthanide luminescence quantum yields (Φ) of 26% and 23%, respectively. The value obtained for **TCS1** is slightly exceeding or comparable to the values for other Tb(III) based Cu^{2+} ion sensors (Φ ≤ 22%).[44] **TCS1** is significantly quenched upon addition of 1 equivalent of Cu^{2+} ions with a Φ of only ~5% in H_2O indicating its potential as a 'turn-off' Cu^{2+} ion sensor.

The long luminescence lifetimes (τ) of **TCS1** and **TCS2** of more than 1 ms in H_2O allow for time-gated experiments to omit background noise and autofluorescence from biological media for improved signal sensitivity. The values for τ are listed in Table 1 along with other photophysical properties and the plots of the emission (measured at 545 nm) vs. time are shown in Figure S12. τ is longer in D_2O than H_2O what was expected because of the less efficient luminescence quenching of O–D oscillators as compared to O–H oscillators in the hydration sphere of Tb(III) allowing to assess the hydration state of the complexes.[59,60] By comparing τ in D_2O and H_2O using Horrocks' and Beeby's empirical models,[59,60] the q number was determined for **1**, **TCS1**, **TCS2** to be 1.3±0.3, 0.8±0.1 and 1.5±0.3. The values of **1** and **TCS1** are consistent with values for monohydrated complexes.[55] The q number of **TCS**2, however, is unusually high and rather suggests coordination of a mixture of one to two molecules of H_2O. Here, it should be noted that the reliability of the determined q number might be compromised due to possible additional deactivation paths of the Tb(III) excited state by Cu^{2+} ions. The slightly lower value of **TCS1** in comparison to the other two complexes might result from the labile coordination of one carboxylate group of the uncoordinated NOTA-moiety to Tb(III) affecting the q number by the relative k_{on}/k_{off} rate.

Table 1. Photophysical properties of **1**, **TCS1** and **TCS2**.

	Absorption λ_{max} (nm) (ε ($\times 10^3$ $M^{-1}cm^{-1}$))		Φ_{ACN} (%)	Φ_{H2O}[a] (%)	τ_{H2O}[a] (ms)	τ_{D2O}[a] (ms)	q[b]
	CH_3CN	H_2O[a]					
1	291 (10.1) 338 (10.7) 349 (8.7)	287 (10.9) 332 (14.8) 346 (12.6)	6.3	26	$1.41^{\pm 8\%}$	$2.58^{\pm 7\%}$	$1.3^{\pm 0.3}$
TCS1	289 (9.0) 339 (9.1) 352 (7.6)	287 (10.1) 333 (12.1) 347 (10.0)	-	23	$1.13^{\pm 1\%}$	$1.51^{\pm 1\%}$	$0.8^{\pm 0.1}$
TCS2	289 (13.6) 337 (9.9) 350 (7.7)	286 (13.0) 333 (12.3) 347 (9.9)	< 0.1	4.9	$1.03^{\pm 6\%}$	$1.62^{\pm 3\%}$	$1.5^{\pm 0.3}$

Quantum yields and lifetimes were measured under excitation at 330 nm at r.t. and a relative error of 10% is typically found among different measurements on the same sample. The errors of the regression are displayed in superscript. [a] Measured in unbuffered solutions at pH 4.5–5.3. [b] q values were estimated using the equation $q = 5$ ($\tau_{H2O} - \tau_{D2O} - 0.06$), allowing for the contribution of unbound water molecules.[59,60] The errors calculated based on the uncertainties in lifetimes are displayed in superscript.

Analysis of pH effects

The luminescence emission of **TCS1** was stable over the pH range of 2–8 with a $pK_a > 9.0$, which most probably corresponds to the deprotonation of the 7-amido NH of the sensitizing chromophore (Figure 2).[55,58] Similarly, at pH > 9, a deprotonation of the metal bound water in the Tb(III) coordination sphere can also occur, which would significantly increase the quenching effect originating from O–H bond oscillations.[58]

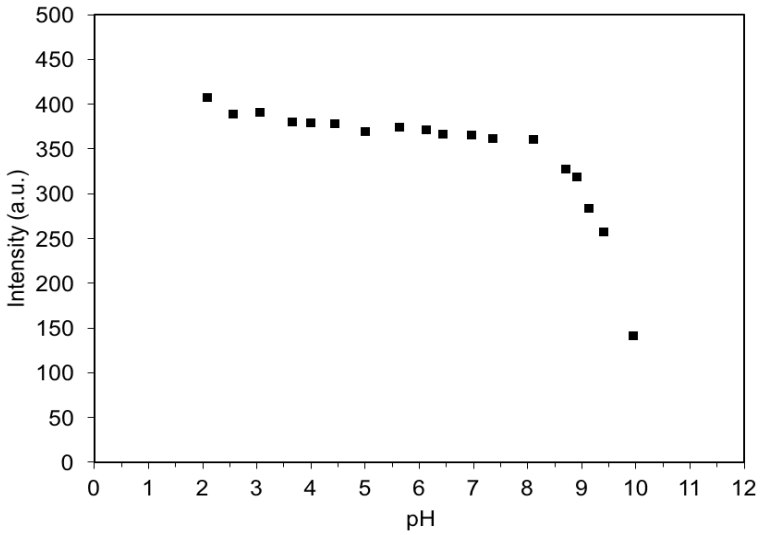

Figure 2. Luminescence response of **TCS1** to changes in pH (2–10) acquired in water (λ_{ex} = 330 nm, λ_{em} = 545 nm).

Sensing of metal ions and limit of detection

Biological samples contain an abundant number of cations including many that exist at much higher concentrations than copper (e.g. Na^+, K^+, Mg^+ and Ca^{2+} ions). The viability of our probe **TCS1** was therefore evaluated for its selectivity for Cu^{2+} ions over other biologically relevant cations (Fe^{2+}, Mn^{2+}, Zn^{2+}, Na^+, K^+, Mg^{2+}, Ca^{2+}). Binding of Cu^{2+} ions to **TCS1** gave a concomitant strong luminescence quenching effect, whereas no or only minor effects were observed with other cations (Figures 3 and 4). It was previously shown that the $[Cu(NOTA)]^-$ complex shows high thermodynamic stability (log K = 23.33) and fast quantitative formation, even at pH <1.5.[52] The NOTA ligand is very selective for Cu^{2+} ions over alkali and earth alkali metal ions (log K = 2–5 and log K = 7–11, respectively) and moderately selective over other transition metal ions (e.g., log K (Mn^{2+}) = 16.30 and log K (Zn^{2+}) = 22.32).[52] Besides thermodynamic considerations, former studies demonstrated that the complexation of NOTA with Cu^{2+} ions is kinetically preferred over several competing ions, including Zn^{2+}.[52]

Analysis of the luminescence titration profile in Figure 3 strongly indicates that **TCS1** binds Cu^{2+} ions in a 1:1 stoichiometry with the most significant changes in luminescence occurring within 0–1 equivalent of Cu^{2+} ions added. The limit of detection (LOD) of Cu^{2+} ions was calculated based on luminescence titration. A good linear relationship between the luminescence intensity and the Cu^{2+} ion concentration could be obtained in the range of 0.1–1.5 μM (Figure 5). The LOD of **TCS1** was determined to be extremely low at about 1.7 nM based on 3 σ/k (where σ is the standard deviation of the blank measurements and k is the slope of the linear regression line between luminescence intensity versus Cu^{2+} ion concentration). To the best of our knowledge, this is the current lowest LOD for any small molecule sensor for Cu^{2+} ions making **TCS1** particularly interesting for applications where the limit of detection of other methods is not low enough for quantifying Cu^{2+} ions, such as in blood, saliva and other biological samples (e.g., salivary copper levels are ~1 μM[61]).[19,51] Table S2 gives an overview on LODs of other small molecule Cu^{2+} ion sensors.

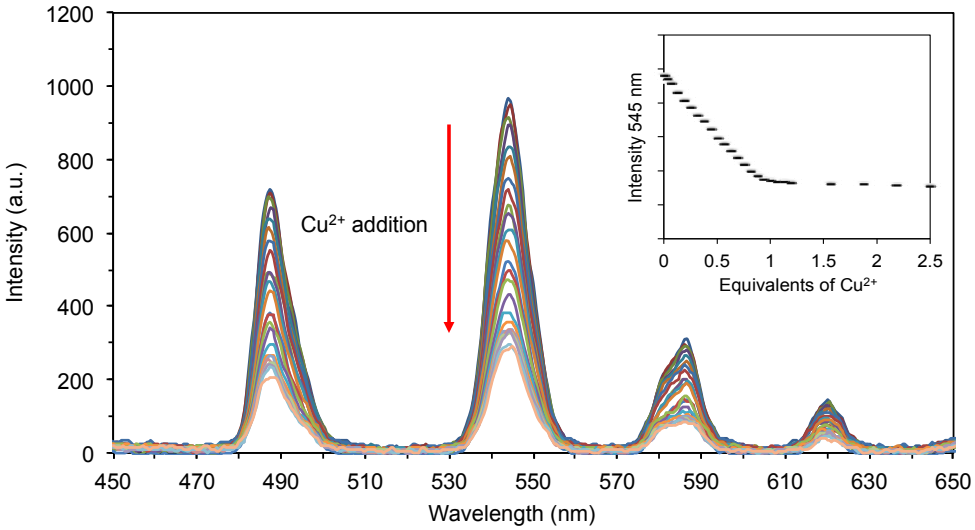

Figure 3. Luminescence emission spectra of **TCS1** (2 μM in H_2O, λ_{ex} = 330 nm) titrated with $CuCl_2$. Inset: Luminescence intensity of **TCS1** at 545 nm versus Cu^{2+} ion concentrations in the range 0–5 μM, plotted as equivalents.

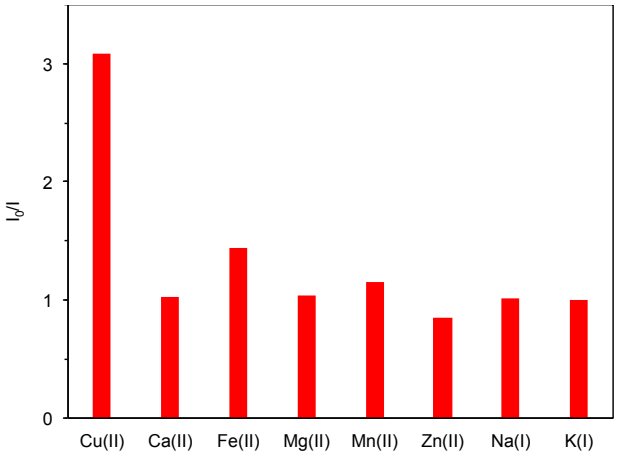

Figure 4. Luminescence response of **TCS1** to various metal ions in H_2O (λ_{ex} = 330 nm, λ_{em} = 545 nm). Bars represent the emission ratio determined by dividing the emission intensity of **TCS1** only (I_0) and **TCS1** after addition of 1 equivalent of metal chloride (I).

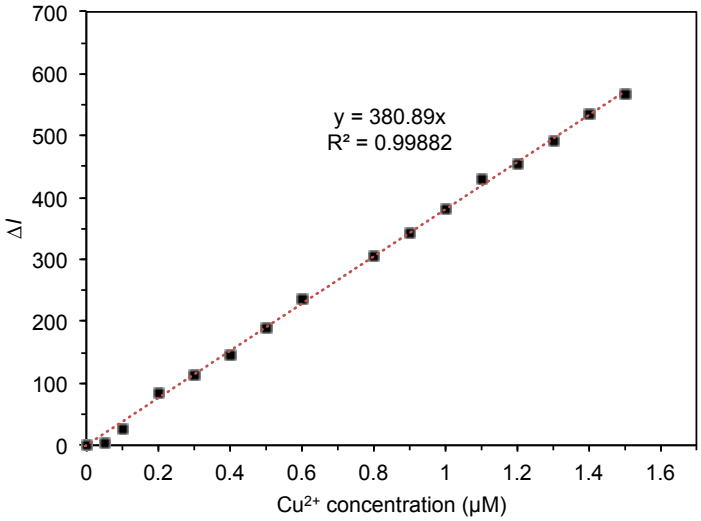

Figure 5. Plot of the quenching intensity (ΔI) versus the concentration of Cu^{2+} ions plotted over the linear range of 0-1.5 μM.

Absorbance titration

Next, the changes in the ground-state properties of **TCS1** upon complexation with Cu^{2+} ions were analyzed via UV/Vis absorbance titration (Figure 6). We observed a small hypsochromic shift of the absorption bands at 255 nm and 287 nm with increasing intensity. The spectrum of $[Cu(NOTA)]^-$ displays an absorption maximum at approximately 270 nm (Cu-N ligand-to-metal charge transfer, LMCT).[52] We thus assume that the spectral changes observed can be attributed to a successful binding of Cu^{2+} ions to the NOTA-moiety.

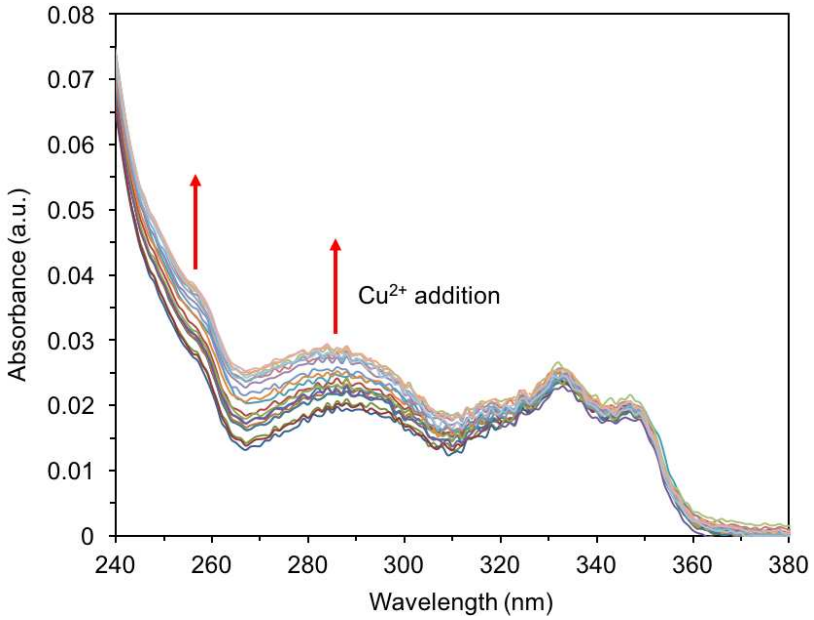

Figure 6. Absorbance spectra of **TCS1** (2 µM in H_2O) titrated with $CuCl_2$ (0–1 equivalent).

Binding constant and quenching mechanism

The apparent binding constant (K_{app}) of **TCS1** to Cu^{2+} ions was determined based on the luminescence quenching observed at 545 nm at pH ≈ 7. Assuming a 1:1 complex formation that is linearly proportional to the luminescence quenching response, non-linear least-squares fit to the titration data gave a value of log K_{app} = (7.7 ± 0.1) (Figure 7a). Clearly, the determined K_{app} is significantly lower than the conditional stability constant for [Cu(nota)]− (log K_{eff} = 17.55 at pH 7.4).[52] It is, however, not plausible that the affinity of the NOTA-moiety to Cu^{2+} ions is affected to such an extent when embedded in the **TCS1** structural framework. We were also unable to extract Cu^{2+} ions from **TCS2** by addition of HS^- what suggests the high stability of the complex (solubility product of CuS $K_{SP} = 6.3 \times 10^{-36}$ mol^2dm^{-6}, see also Supporting Information).[40]

We hypothesized that **TCS1** has two modes of binding for Cu^{2+} ions: 1) fast and practically irreversible complexation of the NOTA-moiety and 2) direct quenching interaction of the NOTA-bound Cu^{2+} with the carbostyril sensitizer upon conformational exchange (Figure 7b). Assuming that only the latter leads to luminescence quenching the equilibrium constant K_{app} would be more indicative for the interaction with the sensitizer. The precise nature of the quenching mechanism is ambiguous and currently under further investigation. Cu^{2+} ions could quench the sensitizer through an energy or electron transfer mechanism. Cyclovoltammetric studies by Kovacs *et al.* on comparable carbostyril model compounds showed that these chromophores are good enough electron donors ($E_{red} \approx -1.7$ V vs. NHE)[55,62] making a reduction of Cu^{2+} ($E_{red} \approx -0.7$ V vs. NHE in NOTA framework)[63] likely to be thermodynamically feasible.

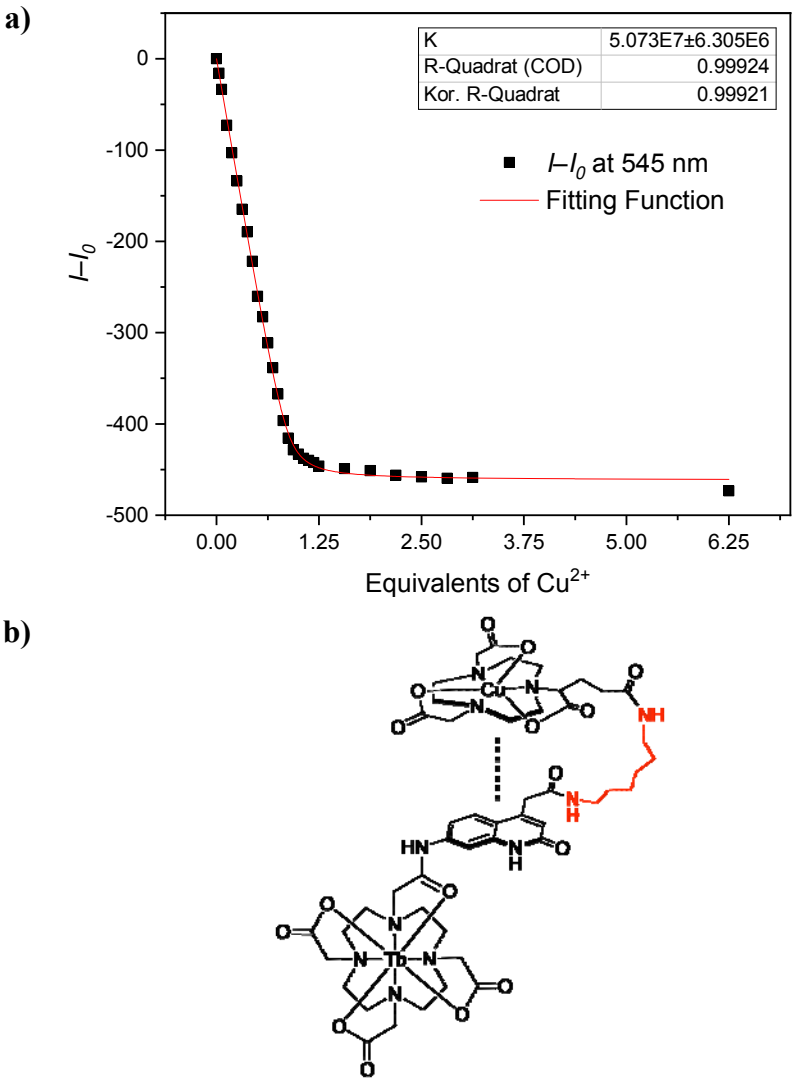

Figure 7. a) Plot of best nonlinear least-squares fit of 1:1 binding model to luminescence Cu^{2+} ion titration data of **TCS1**. I and I_0 are the luminescence intensities at 545 nm in the in the presence and absence of Cu^{2+} ions. **b)** Model of the sensitizer-Cu^{2+} interaction in **TCS2**.

Conclusions

The high luminescence quantum yield and long lifetime of **TCS1** in water are a good basis for the development of luminescent sensors with high optical sensitivity and fidelity to detect Cu^{2+} ions within the low concentration window of biological media. Further advantages for this purpose are its excellent water-solubility and excitation wavelength of up to 350 nm. Since NOTA as receptor moiety binds Cu^{2+} ions in a practically irreversible manner, **TCS1** can function as a chemical trap and potentially provide an accumulative detection for the presence of this ion in the development of biological or analytical assays.

Experimental Section

Materials and reagents

All starting materials, reagents and solvents were obtained from commercial suppliers (Sigma-Aldrich, Fluka, Honeywell) and were of general reagent grade or analytical grade and used without further purification. All solvents were used as received. NODA-GA-NHS ester ($C_{19}H_{28}N_4O_{10}(HPF_6)(CF_3COOH)$) was purchased from CheMatech (Dijon, France).

Instrumentation and methods

^{1}H NMR spectra were recorded at 400 MHz and ^{13}C NMR spectra were recorded at 101 MHz in deuterated solvents at room temperature on a Bruker Avance 400 NMR spectrometer. The chemical shifts (δ) are reported in units of ppm (parts per million) and referenced internally from the residual proteo-solvent resonance. Multiplicities for NMR resonances are abbreviated for reporting; s (singlet), d (doublet), dd (doublet of doublets), t (triplet), q (quartet), m (multiplet), br (broad), ar (aromatic) (Figures S1–S4). Silica gel chromatography was performed using Davisil LC35A10 silica (Grace Davision). Reversed-phase silica gel chromatography was performed using Davisil 70NC18E silica (Grace Davision). Analytical UPLC analyses were performed on a VWR Hitachi Chromaster UPLC instrument equipped with a Waters Acquity UPLC BEH C18 column (1.7 µm, 2.1 × 50 mm). The runs were performed at a flow rate of 0.6 mL/min using a linear gradient of buffer A (distilled water containing 0.1% v/v TFA) and buffer B (CH_3CN, Sigma-Aldrich HPLC grade, containing 0.1% v/v TFA): t = 0–0.5 min (5% B), t = 1.5 min (100% B), t = 2.5 min (100% B). UPLC-MS were measured with a Waters Acquity^{TM} UPLC system equipped with a PDA detector, an auto-sampler and an Acquity UPLC BEH C18 column (1.7 µm, 2.1 × 50 mm) coupled to the Bruker Daltonics HCT 6000 mass spectrometer. The elution method was 0.6 mL/min with a linear gradient of buffer C (double distilled water with 0.1% v/v formic acid) and buffer D (CH_3CN, Sigma-Aldrich UPLC grade, containing 0.1% v/v formic acid): t = 0–0.25 min (5% D), t = 1.5 min (100% D), t = 2.5 min (100% D). HR-MS was performed on a Bruker maXis QTOF high-resolution mass spectrometer (Bruker Daltonics, Bremen, Germany). Analytical RP-HPLC was performed on a VWR Hitachi Chromaster HPLC system (Chromaster HPLC 5430 diode array detector, Chromaster HPLC 5310 column oven, Chromaster HPLC 5210 autosampler and a Chromaster HPLC 5110 pump) with a Macherey Nagel EC 250/3 Nucleosil 100-5 C18 column. The elution method was 0.75 mL/min with a linear gradient of buffer A and buffer B: t = 0–3 min (5% B), t = 20 min (80% B), t = 22 min (100% B).

Preparative HPLC purifications were performed on a Varian Prostar HPLC system using an Agilent Zorbax 300 SB-C18 prep column (5 μm, 150 × 21.2 mm). IR absorption spectra were obtained on a SpectrumTwo FTIR Spectrometer (Perkin–Elmer) equipped with a Specac Golden Gate™ ATR (attenuated total reflection) accessory. Elemental microanalyses were performed on a LecoCHNS-932 elemental analyzer.

Syntheses

Synthesis of 1: The procedure was adapted from the reported synthesis of the Eu(III) analogue with the substitution of $Eu(OTf)_3$ for $Tb(OTf)_3$ (see Supporting Information).[57,58] **1** was isolated as a TFA salt. Analytical UPLC (C18, 275 nm): R_t = 1.20 min; UPLC-MS (C18, 275 nm): R_t (*m/z*) = 0.70 min (761.3 $[M+H]^+$, 381.1 $[M+2H]^{2+}$); HR-MS (*m/z*): calcd for $C_{27}H_{34}N_6O_{10}Tb$ $[M+H]^+$ 761.15844, found: 761.15816. IR (neat; 4000–600 cm^{-1}): ν_{max} = 2879*w*, 1588*s*, 1462*w*, 1405*w*, 1318*w*, 1179*m*, 1083*m*, 1002*w*, 971*w*, 935*w*, 823*m*, 677*s*, 618*m*. Elemental analysis calc. for $C_{27}H_{33}N_6O_8Tb$ (CF_3COOH) $(H_2O)_2$ (%): C, 38.25; H, 4.21; N, 9.23; found: C, 37.95; H, 4.60; N, 9.36.

Synthesis of 2: Complex **1** (25 mg, 0.027 nmol) was dissolved in DMSO (5 mL) and to this mixture was added Et_3N (11 mg, 15 μL, 0.11 mmol), HATU (42 mg, 0.11 mmol) and 1,6-diaminohexane (6.5 mg, 0.055 mmol). The solution was stirred for 17 h at *r.t.* and then purified by preparative HPLC. The combined fractions were lyophilized to afford a white powder. Yield: 22 mg, 0.025 mmol, 93%. Analytical UPLC (C18, 275 nm): R_t = 1.22 min; UPLC-MS (C18, 275 nm): R_t (*m/z*) = 0.78 min (430.3 $[M+2H]^{2+}$, 859.3 $[M+H]^+$); HR-MS (*m/*z): calc. for $C_{33}H_{48}N_8O_9Tb$ $[M+H]^+$ 859.27922, found: 859.27875. IR (neat, 4000–600 cm^{-1}): ν_{max} = 3295*w*, 3084*w*, 2937*w*, 2868*w*, 1587*s*, 1558*m*, 1458*w*, 1403*m*, 1319*w*, 1199*s*, 1178*s*, 1128*s*, 1083*s*, 1002*w*, 969*w*, 939*w*, 905*w*, 885*w*, 834*m*, 799*m*, 719*s*, 663*w*.

Synthesis of TCS1: Complex **2** (20 mg, 0.023 mmol) was dissolved in DMF (5 mL) and to this mixture was added NODA-GA-NHS ester (28 mg, 0.038 mmol) and Et_3N (10 mg, 14 μL, 0.10 mmol). The solution was stirred for 20 h at *r.t.* and then purified by preparative HPLC. The combined fractions were lyophilized to afford the product as a TFA salt (white powder). Yield: 12 mg, 9.9 μmol, 43%. Analytical UPLC (C18, 275 nm): R_t = 1.29 min; UPLC-MS (C18, 275 nm): R_t (*m/z*) = 0.77 min (608.9 $[M+2H]^{2+}$, 1216.5 $[M+H]^+$); HR-MS (*m/z*): calc. for $C_{48}H_{72}N_{11}O_{16}Tb$ $[M+2H]^{2+}$ 608.72005, found: 608.72098. IR (neat, 3500–600 cm^{-1}): ν_{max} = 2987*w*, 2884*w*, 1653*s*, 1617*s*, 1592*s*, 1554*m*, 1459w, 1404*w*, 1321*w*, 1246*w*, 1176*s*, 1127*s*, 1084*w*, 969*w*, 938*w*, 886*w*, 831*w*, 798*m*, 719*s*, 680*m*, 667*m*. Elemental analysis calc. for

$C_{48}H_{70}N_{11}O_{16}Tb$ $(CF_3COOH)_{1.5}$ $(H_2O)_2$ (%): C, 43.04; H, 5.35; N, 10.83; found: C, 43.34; H, 5.74; N, 10.57.

Spectroscopic studies

UV/Vis absorbance spectra were measured on an Agilent Cary 8454 UV/Vis spectrophotometer or a Specord 250 Plus spectrophotometer (Analystik Jena AG). Emission spectra and lifetimes were measured on a Perkin Elmer LS50B luminescence spectrometer with a xenon discharge lamp (equivalent to 20 kW for 8 µs duration and pulse width at half height <10 µs) and a gated photomultiplier with modified S5 response for operation up to around 650 nm as detector. All spectroscopic studies were performed in spectroscopic grade solvents using quartz cells with 1 cm optical pathlength at r.t. Luminescence quantum yields were determined by a comparative method relative to quinine sulfate (in 0.1 M H_2SO_4; Φ_{ref} = 0.54)[64–66] for the measurements in CH_3CN and anthracene (in EtOH; Φ_{ref} = 0.27)[64] for the measurements in H_2O. The samples of similar absorbance (< 0.5 at λ_{ex}) were excited at 330 nm with constant slit widths (Ex 4.0 nm, Em 4.5 nm) measured over 350–800 nm (t_{delay} = 0 ms). Absorbance and emission spectra were measured from the same solutions and the absorbance at 330 nm was plotted against the integrated luminescence signal for linear regression analysis. The quantum yield (Φ_x) was calculated using Φ_{ref} and the gradients of the linear regressions of the sample ($grad_x$) and reference ($grad_{ref}$) and corrected for differences in the refractive indices of the solvents for the sample (n_x) and reference (n_{ref}) as per:

$$\Phi_x = \Phi_{ref}\left(\frac{\mathrm{grad}_x}{\mathrm{grad}_{ref}}\right)\left(\frac{{n_x}^2}{{n_{ref}}^2}\right)$$

Lifetimes were determined by measuring the emission intensity at 545 nm for at least 7 different delay times between t_{delay} = 0.05–0.8 ms. The obtained data was fitted with Microsoft Excel software (Microsoft Corporation, Redmond, WA, USA) assuming mono-exponential decay. The corresponding graphs can be found in Figure S12. The hydration numbers (q) were calculated from the difference in lifetimes in H_2O and D_2O using q = 5 ($\tau_{H2O}^{-1} - \tau_{D2O}^{-1} - 0.06$). The errors given on the q values were calculated based on the error in the regression of the lifetime data using error propagation theory (Table S1). A relative error of 10% is typically found among different quantum yield and lifetime measurements on the same sample.

Determination of binding constant

The binding constant (K_a) of ground state 1:1 luminophore–quencher complex (LQ) can be determined by non-linear least-square fitting (Origin software, OriginLab Corporation, Northampton, MA, USA) of the luminescence change vs. quencher concentration data according to the mathematical model below.[67]

$$(I - I_0) = -A\,[\mathrm{LQ}]$$

$$[\mathrm{LQ}] = \frac{\left(\frac{1}{K_a} + [\mathrm{L}]_0 + [\mathrm{Q}]_0\right) - \sqrt{\left(\frac{1}{K_a} + [\mathrm{L}]_0 + [\mathrm{Q}]_0\right)^2 - 4[\mathrm{L}]_0[\mathrm{Q}]_0}}{2}$$

I and I_0 are the luminescence intensities at 545 nm in the presence and absence of Cu^{2+} ions and A is the change in proportionality constant between the free ligand and LQ. $[L]_0$ and $[Q]_0$ are the known total concentrations of **TCS1** and Cu^{2+} ions respectively.

Associated content

Supporting information for this article is available on the WWW under http://dx.doi.org/

Author information

Corresponding Authors:

* E-mail: gilles.gasser@chimie-paristech.fr (G.G.)

* Website: www.gassergroup.com (G.G.)

ORCID

Franz Heinemann: 0000-0001-9590-443X

Michèle Clerc: 0000-0003-3252-5410

Bernhard Spingler: 0000-0003-3402-2016

Gilles Gasser: 0000-0002-4244-5097

Notes:

The authors declare no competing financial interest.

Acknowledgements

We gratefully thank Dr. Phuc Ung, who was funded by a Victorian Postdoctoral Research Fellowship and the Humboldt Foundation, for his contributions to this work. We thank Prof. Dr. K. Eszter Borbas for helpful comments to the manuscript. This work was supported by the program «Investissements d'Avenir» launched by the French Government and implemented by the ANR with the reference ANR-10-IDEX-0001-02 PSL (G.G.).

References

(1) Barceloux, D. G. Copper. *J. Toxicol. - Clin. Toxicol.* **1999**, *37*, 217–230.
(2) Kim, B.-E.; Nevitt, T.; Thiele, D. J. Mechanisms For Copper Acquisition, Distribution And Regulation. *Nat. Chem. Biol.* **2008**, *4*, 176–185.
(3) Festa, R. A.; Thiele, D. J. Copper: An Essential Metal In Biology. *Curr. Biol.* **2011**, *21*, R877–R883.
(4) Finney, L.; Vogt, S.; Fukai, T.; Glesne, D. Copper And Angiogenesis: Unravelling A Relationship Key To Cancer Progression. *Clin. Exp. Pharmacol. Physiol.* **2009**, *36*, 88–94.
(5) Xiao, T.; Ackerman, C. M.; Carroll, E. C.; Jia, S.; Hoagland, A.; Thai, B.; Liu, C. S.; Isacoff, E. Y.; Chang, C. J. Copper Regulates Rest-Activity Cycles Through The Locus Coeruleus-Norepinephrine System. *Nat. Chem. Biol.* **2018**, *14*, 655–663.
(6) Ackerman, C. M.; Chang, C. J. Copper Signaling In The Brain And Beyond. *J. Biol. Chem.* **2018**, *293*, 4628–4635.
(7) McMillin, G. A.; Travis, J. J.; Hunt, J. W. Direct Measurement Of Free Copper In Serum Or Plasma Ultrafiltrate. *Am. J. Clin. Pathol.* **2009**, *131*, 160–165.
(8) Huang, P.; Wu, F.; Mao, L. Target-Triggered Switching On And Off The Luminescence Of Lanthanide Coordination Polymer Nanoparticles For Selective And Sensitive Sensing Of Copper Ions In Rat Brain. *Anal. Chem.* **2015**, *87*, 6834–6841.
(9) Forzani, E. S.; Zhang, H.; Chen, W.; Tao, N. Detection Of Heavy Metal Ions In Drinking Water Using A High-Resolution Differential Surface Plasmon Resonance Sensor. *Environ. Sci. Technol.* **2005**, *39*, 1257–1262.
(10) Urban, R. C.; Romero, J. R.; Campos, M. L. A. M. Development Of A Portable Sensor To Evaluate Copper Speciation In Natural Waters. *Anal. Methods* **2018**, *10*, 2056–2063.
(11) Chan, M.-S.; Huang, S.-D. Direct Determination Of Cadmium And Copper In Seawater Using A Transversely Heated Graphite Furnace Atomic Absorption Spectrometer With Zeeman-Effect Background Corrector. *Talanta* **2000**, *51*, 373–380.
(12) Cotruvo, J. A.; Aron, A. T.; Ramos-Torres, K. M.; Chang, C. J. Synthetic Fluorescent Probes For Studying Copper In Biological Systems. *Chem. Soc. Rev.* **2015**, *44*, 4400–4414.
(13) Dodani, S. C.; Domaille, D. W.; Nam, C. I.; Miller, E. W.; Finney, L. A.; Vogt, S.; Chang, C. J. Calcium-Dependent Copper Redistributions In Neuronal Cells Revealed By A Fluorescent Copper Sensor And X-Ray Fluorescence Microscopy. *PNAS* **2011**, *108*, 5980–5985.
(14) Dodani, S. C.; Leary, S. C.; Cobine, P. A.; Winge, D. R.; Chang, C. J. A Targetable Fluorescent Sensor Reveals That Copper-Deficient SCO1 And SCO2 Patient Cells Prioritize Mitochondrial Copper Homeostasis. *J. Am. Chem. Soc.* **2011**, *133*, 8606–8616.
(15) Domaille, D. W.; Zeng, L.; Chang, C. J. Visualizing Ascorbate-Triggered Release Of Labile Copper Within Living Cells Using A Ratiometric Fluorescent Sensor. *J. Am. Chem. Soc.* **2010**, *132*, 1194–1195.
(16) Hirayama, T.; Bittner, G. C. Van De; Gray, L. W.; Lutsenko, S.; Chang, C. J. Near-Infrared Fluorescent Sensor For In Vivo Copper Imaging In A Murine Wilson Disease Model. *PNAS* **2012**, *109*, 2228–2233.
(17) Huang, C. P.; Fofana, M.; Chan, J.; Chang, C. J.; Howell, S. B. Copper Transporter 2 Regulates Intracellular Copper And Sensitivity To Cisplatin. *Metallomics* **2014**, *6*, 654–661.
(18) Wu, J.; Boyle, E. A. Low Blank Preconcentration Technique For The Determination Of Lead, Copper, And Cadmium In Small-Volume Seawater Samples By Isotope Dilution ICPMS. *Anal. Chem.* **1997**, *69*, 2464–2470.
(19) Chen, H.; Jia, S.; Zhang, J.; Jang, M.; Chen, X.; Koh, K.; Wang, Z. Sensitive Detection Of Copper(II) Ions Based On The Conformational Change Of Peptides By Surface Plasmon Resonance Spectroscopy. *Anal. Methods* **2015**, *7*, 8942–8946.
(20) Liu, Y.; Liang, P.; Guo, L. Nanometer Titanium Dioxide Immobilized On Silica Gel As Sorbent For Preconcentration Of Metal Ions Prior To Their Determination By Inductively Coupled Plasma Atomic Emission Spectrometry. *Talanta* **2005**, *68*, 25–30.
(21) Kimmel, D. W.; Leblanc, G.; Meschievitz, M. E.; Cliffel, D. E. Electrochemical Sensors And Biosensors. *Anal. Chem.* **2012**, *84*, 685–707.
(22) Saleem, M.; Rafiq, M.; Hanif, M.; Shaheen, M. A.; Seo, S. Y. A Brief Review On Fluorescent Copper Sensor Based On Conjugated Organic Dyes. *J. Fluoresc.* **2018**, *28*, 97–165.
(23) Zhao, M.; Yang, X. F.; He, S.; Wang, L. A Rhodamine-Based Chromogenic And Fluorescent Chemosensor For Copper Ion In Aqueous Media. *Sensors Actuators, B Chem.* **2009**, *135*, 625–631.
(24) Zhang, J.; Zhao, B.; Li, C.; Zhu, X.; Qiao, R. A BODIPY-Based "Turn-On" Fluorescent And Colorimetric Sensor For Selective Detection Of Cu2+ In Aqueous Media And Its Application In Cell Imaging. *Sensors Actuators, B Chem.* **2014**, *196*, 117–122.
(25) Shen, C.; Kolanowski, J. L.; Tran, C. M.-N.; Kaur, A.; Akerfeldt, M. C.; Rahme, M. S.; Hambley, T.

W.; New, E. J. A Ratiometric Fluorescent Sensor For The Mitochondrial Copper Pool. *Metallomics* **2016**, *8*, 915–919.
(26) Dai, Q.; Liu, H.; Gao, C.; Li, W.; Zhu, C.; Lin, C.; Tan, Y.; Yuan, Z.; Jiang, Y. A One-Step Synthesized Acridine-Based Fluorescent Chemosensor For Selective Detection Of Copper (II) Ions And Living Cell Imaging. *New J. Chem.* **2018**, *42*, 613–618.
(27) Morgan, M. T.; McCallum, A. M.; Fahrni, C. J. Rational Design Of A Water-Soluble, Lipid-Compatible Fluorescent Probe For Cu(I) With Sub- Part-Per-Trillion Sensitivity. *Chem. Sci.* **2016**, *7*, 1468–1473.
(28) Cody, J.; Fahrni, C. J. Fluorescence Sensing Based On Cation-Induced Conformational Switching : Copper-Selective Modulation Of The Photoinduced Intramolecular Charge Transfer Of A Donor – Acceptor Biphenyl Fluorophore. *Tetrahedron* **2004**, *60*, 11099–11107.
(29) Chaudhry, A. F.; Verma, M.; Morgan, M. T.; Henary, M. M.; Siegel, N.; Hales, J. M.; Perry, J. W.; Fahrni, C. J. Kinetically Controlled Photoinduced Electron Transfer Switching In Cu (I) -Responsive Fluorescent Probes. *J. Am. Chem. Soc.* **2010**, *132*, 737–747.
(30) Fabbrizzi, L.; Licchelli, M.; Pallavicini, P.; Perotti, A.; Taglietti, A.; Sacchi, D.; Abstract: Fluorescent Sensors For Transition Metals Based On Electron-Transfer And Energy-Transfer Mechanisms. *Chem. Eur. J.* **1996**, *2*, 1–9.
(31) Fabbrizzi, L.; Licchelli, M.; Pallavicini, P.; Sacchi, D.; Taglietti, A. Sensing Of Transition Metals Through Fluorescence Quenching Or Enhancement. *Analyst* **1996**, *121*, 1763–1768.
(32) Bünzli, J. –C. G. On The Design Of Highly Luminescent Lanthanide Complexes. *Coord. Chem. Rev.* **2015**, *293–294*, 19–47.
(33) Mathieu, E.; Sipos, A.; Demeyere, E.; Phipps, D.; Sakaveli, D.; Borbas, K. E. Lanthanide-Based Tools For The Investigation Of Cellular Environments. *Chem. Commun.* **2018**, *54*, 10021–10035.
(34) Meshkova, S. B.; Topilova, Z. M.; Gorodnyuk, V. P.; Kiriyak, A. V; Antonovich, V. P.; Andrianov, A. M. Sensitization Of The 4f-Luminescence Of Terbium With Copper Ions And Its Analytical Application. *J. Anal. Chem.* **2004**, *59*, 945–949.
(35) Viguier, R. F. H.; Hulme, A. N. A Sensitized Europium Complex Generated By Micromolar Concentrations Of Copper(I): Toward The Detection Of Copper(I) In Biology. *J. Am. Chem. Soc.* **2006**, *128*, 11370–11371.
(36) Nonat, A. M.; Harte, A. J.; Sénéchal-David, K.; Leonard, J. P.; Gunnlaugsson, T. Luminescent Sensing And Formation Of Mixed F–D Metal Ion Complexes Between A Eu(III)-Cyclen-Phen Conjugate And Cu(II), Fe(II), And Co(II) In Buffered Aqueous Solution. *J. Chem. Soc. Dalton Trans.* **2009**, No. 24, 4703–4711.
(37) McMahon, B. K.; Gunnlaugsson, T. Lanthanide Luminescence Sensing Of Copper And Mercury Ions Using An Iminodiacetate-Based Tb(III)-Cyclen Chemosensor. *Tetrahedron Lett.* **2010**, *51*, 5406–5410.
(38) Golovach, Y. P.; Kiriyak, A. V.; Ognichenko, L. N.; Basok, S. S.; Kovalevskaya, I. P.; Rakipov, I. M.; Kuz'min, V. E.; Meshkova, S. B. The Role Of Copper Ions In Tb(III) Luminescence Sensitization In Heterometallic Complexes With Podands. *Russ. J. Inorg. Chem.* **2016**, *61*, 872–876.
(39) Yip, Y.-W.; Law, G.-L.; Wong, W.-T. A Highly Selective On–Off–On Responsive Lanthanide(III) Based Probe For Recognition Of Copper And Hydrogen Sulfide. *Dalton Trans.* **2016**, *45*, 928–935.
(40) Liang, Z.; Tsoi, T.-H.; Chan, C.-F.; Dai, L.; Wu, Y.; Du, G.; Zhu, L.; Lee, C.-S.; Wong, W.-T.; Law, G.-L.; Wong, K.-L. A Smart "Off–On" Gate For The In Situ Detection Of Hydrogen Sulphide With Cu(II)-Assisted Europium Emission. *Chem. Sci.* **2016**, *7*, 2151–2156.
(41) Eliseeva, S. V.; Golovach, I. P.; Liasotskyi, V. S.; Antonovich, V. P.; Petoud, S.; Meshkova, S. B. A Role Of Copper(II) Ions In The Enhancement Of Visible And Near-Infrared Lanthanide(III) Luminescence. *J. Lumin.* **2016**, *171*, 191–197.
(42) Wang, Y.; Wang, H.; Zhao, X.; Jin, Y.; Xiong, H.; Yuan, J.; Wu, J. A β-Diketonate-Europium(III) Complex-Based Fluorescent Probe For Highly Sensitive Time-Gated Luminescence Detection Of Copper And Sulfide Ions In Living Cells. *New J. Chem.* **2017**, *41*, 5981–5987.
(43) Hanna, J. R.; Allan, C.; Lawrence, C.; Meyer, O.; Wilson, N. D.; Hulme, A. N. Optimizing The Readout Of Lanthanide-DOTA Complexes For The Detection Of Ligand-Bound Copper(I). *Molecules* **2017**, *22*, 802.
(44) Aulsebrook, M. L.; Biswas, S.; Leaver, F. M.; Grace, M. R.; Graham, B.; Barrios, A. M.; Tuck, K. L. A Luminogenic Lanthanide-Based Probe For The Highly Selective Detection Of Nanomolar Sulfide Levels In Aqueous Samples. *Chem. Commun.* **2017**, *53*, 4911–4914.
(45) Isaac, M.; Denisov, S. A.; Roux, A.; Imbert, D.; Jonusauskas, G.; McClenaghan, N. D.; Sénèque, O. Lanthanide Luminescence Modulation By Cation-π Interaction In A Bioinspired Scaffold: Selective Detection Of Copper(I). *Angew. Chem. Int. Ed.* **2015**, *54*, 11453–11456.
(46) Barja, B. C.; Bari, S. E.; Marchi, M. C.; Iglesias, F. L.; Bernardi, M. Luminescent Eu(III) Hybrid Sensors For In Situ Copper Detection. *Sensors Actuators B* **2011**, *158*, 214–222.

(47) Barja, B. C.; Remorino, A.; Aramendía, P. F. Luminescence Quenching Of Eu(III) Carboxylates By Cu(II) In A Composite Polymer Xerogel Film. *Photochem. Photobiol.* **2006**, *82*, 43–49.
(48) Tang, K.; Ma, Q.; Zhan, Q.; Wang, Q. An Intelligent Copper(II) Luminescent Sensor Using Europium Narrow Emissions Based On Titania Hybrid Material. *Opt. Mater.* **2014**, *36*, 1520–1524.
(49) Cao, F.; Yuan, Z.; Liu, J.; Ling, J. Europium(III) β-Diketone Complex As Portable Luminescent Chemosensor For Naked Eye Cu^{2+} Detection And Recyclable On–Off–On Vapor Response. *RSC Adv.* **2015**, *5*, 102535–102541.
(50) Su, R.; Gao, J.; Deng, S.; Zhang, R.; Zheng, Y. Dual-Target Optical Sensors Assembled By Lanthanide Complex Incorporated Sol–Gel-Derived Polymeric Films. *J. Sol-Gel Sci. Technol.* **2016**, *78*, 606–612.
(51) Aulsebrook, M. L.; Graham, B.; Grace, M. R.; Tuck, K. L. Lanthanide Complexes For Luminescence-Based Sensing Of Low Molecular Weight Analytes. *Coord. Chem. Rev.* **2018**, *375*, 191–220.
(52) Kubíček, V.; Böhmová, Z.; Ševčíková, R.; Vaněk, J.; Lubal, P.; Poláková, Z.; Michalicová, R.; Kotek, J.; Hermann, P. NOTA Complexes With Copper(II) And Divalent Metal Ions: Kinetic And Thermodynamic Studies. *Inorg. Chem.* **2018**, *57*, 3061–3072.
(53) Navarro, A.-S.; Bihan, T. Le; Saëc, P. Le; Bris, N. Le; Bailly, C.; Saï-Maurel, C.; Bourgeois, M.; Chérel, M.; Tripier, R.; Faivre-Chauvet, A. TE1PA As Innovating Chelator For 64 Cu Immuno-TEP Imaging: A Comparative In Vivo Study With DOTA/NOTA By Conjugation On 9E7.4 MAb In A Syngeneic Multiple Myeloma Model′. *Bioconjugate Chem.* **2019**, *30*, 2393–2403.
(54) Maheshwari, V.; Dearling, J. L. J.; Treves, S. T.; Packard, A. B. Measurement Of The Rate Of Copper(II) Exchange For 64Cu Complexes Of Bifunctional Chelators. *Inorg. Chim. Acta* **2012**, *393*, 318–323.
(55) Kovacs, D.; Lu, X.; Mészáros, L. S.; Ott, M.; Andres, J.; Borbas, K. E. Photophysics Of Coumarin And Carbostyril-Sensitized Luminescent Lanthanide Complexes: Implications For Complex Design In Multiplex Detection. *J. Am. Chem. Soc.* **2017**, *139*, 5756–5767.
(56) Kovacs, D.; Phipps, D.; Orthaber, A.; Borbas, K. E. Highly Luminescent Lanthanide Complexes Sensitised By Tertiary Amide-Linked Carbostyril Antennae. *Dalton Trans.* **2018**, *47*, 10702–10714.
(57) Jenie, S. N. A.; Du, Z.; McInnes, S. J. P.; Ung, P.; Graham, B.; Plush, S. E.; Voelcker, N. H. Biomolecule Detection In Porous Silicon Based Microcavities Via Europium Luminescence Enhancement. *J. Mater. Chem. B* **2014**, *2*, 7694–7703.
(58) Jenie, S. N. A.; Hickey, S. M.; Du, Z.; Sebben, D.; Brooks, D. A.; Voelcker, N. H.; Plush, S. E. A Europium-Based 'Off-On' Colourimetric Detector Of Singlet Oxygen. *Inorganica Chim. Acta* **2017**, *462*, 236–240.
(59) Horrocks, W. D.; Sudnick, D. R. Lanthanide Ion Probes Of Structure In Biology. Laser-Induced Luminescence Decay Constants Provide A Direct Measure Of The Number Of Metal-Coordinated Water Molecules. *J. Am. Chem. Soc.* **1979**, *490*, 334–340.
(60) Beeby, A.; Clarkson, I. M.; Dickins, R. S.; Faulkner, S.; Parker, D.; Royle, L.; de Sousa, A. S.; Williams, J. A. G.; Woods, M. Non-Radiative Deactivation Of The Excited States Of Europium, Terbium And Ytterbium Complexes By Proximate Energy-Matched OH, NH And CH Oscillators: An Improved Luminescence Method For Establishing Solution Hydration States. *J. Chem. Soc., Perkin Trans.* **1999**, *2*, 493–503.
(61) Brody, T. Inorganic Nutrients. In *Nutritional Biochemistry*; Academic Press: San Diego, 1999; pp 693–878.
(62) Kovacs, D.; Borbas, K. E. The Role Of Photoinduced Electron Transfer In The Quenching Of Sensitized Europium Emission. *Coord. Chem. Rev.* **2018**, *364*, 1–9.
(63) Wadas, T. J.; Wong, E. H.; Weisman, G. R.; Anderson, C. J. Coordinating Radiometals Of Copper, Gallium, Indium, Yttrium And Zirconium For PET And SPECT Imaging Of Disease. *Chem Rev.* **2010**, *110*, 2858–2902.
(64) Melhuish, W. H. Quantum Efficiencies Of Fluorescence Of Organic Substances: Effect Of Solvent And Concentration Of The Fluorescent Solute. *J. Phys. Chem.* **1961**, *65*, 229–235.
(65) Lakowicz, J. R. *Principles of Fluorescence Spectroscopy*, 3rd ed.; Lakowicz, J. R., Ed.; Springer: New York, 2006.
(66) Velapoldi, R. A. Considerations On Organic Compounds In Solution And Inorganic Ions In Glasses As Fluorescent Standard Reference Materials. *J. Res. Natl. Bur. Stand. Sect. A Phys. Chem.* **1972**, *76A*, 641–654.
(67) Thordarson, P. Determining Association Constants From Titration Experiments In Supramolecular Chemistry. *Chem. Soc. Rev.* **2011**, *40*, 1305–1323.